

Characterisation of Anderson localisation using distributions



A. Alvermann^{1,2}, G. Schubert², A. Weiße³, F.X. Bronold², H. Fehske²

¹Regionales Rechenzentrum Erlangen, Universität Erlangen, Germany

²Institut für Physik, Universität Greifswald, Germany

³School of Physics, The University of New South Wales, Sydney, Australia



We examine the use of distributions in numerical treatments of Anderson localisation and demonstrate how a formulation based on the distribution of the local density of states can be used to study the localisation properties of a single Holstein polaron.

Introduction

When studying Anderson localisation in interacting systems the crucial question is which localisation criterion should be employed. In his pioneering work [1] P.W. Anderson supported to focus on the *distribution* of local quantities as the local density of states (LDOS). Although the distribution of the LDOS should be understood as the primary object of the approach presented here the localisation transition itself will be detected through an appropriately averaged quantity which does account for the qualitative difference of the LDOS in the regime of extended and localised states.

Localisation in the Anderson model

As the generic model for localisation of a single electron in a system with substitutional disorder we consider the Anderson model

$$H = \sum_i \epsilon_i c_i^\dagger c_i + t \sum_{\langle i,j \rangle} c_i^\dagger c_j$$

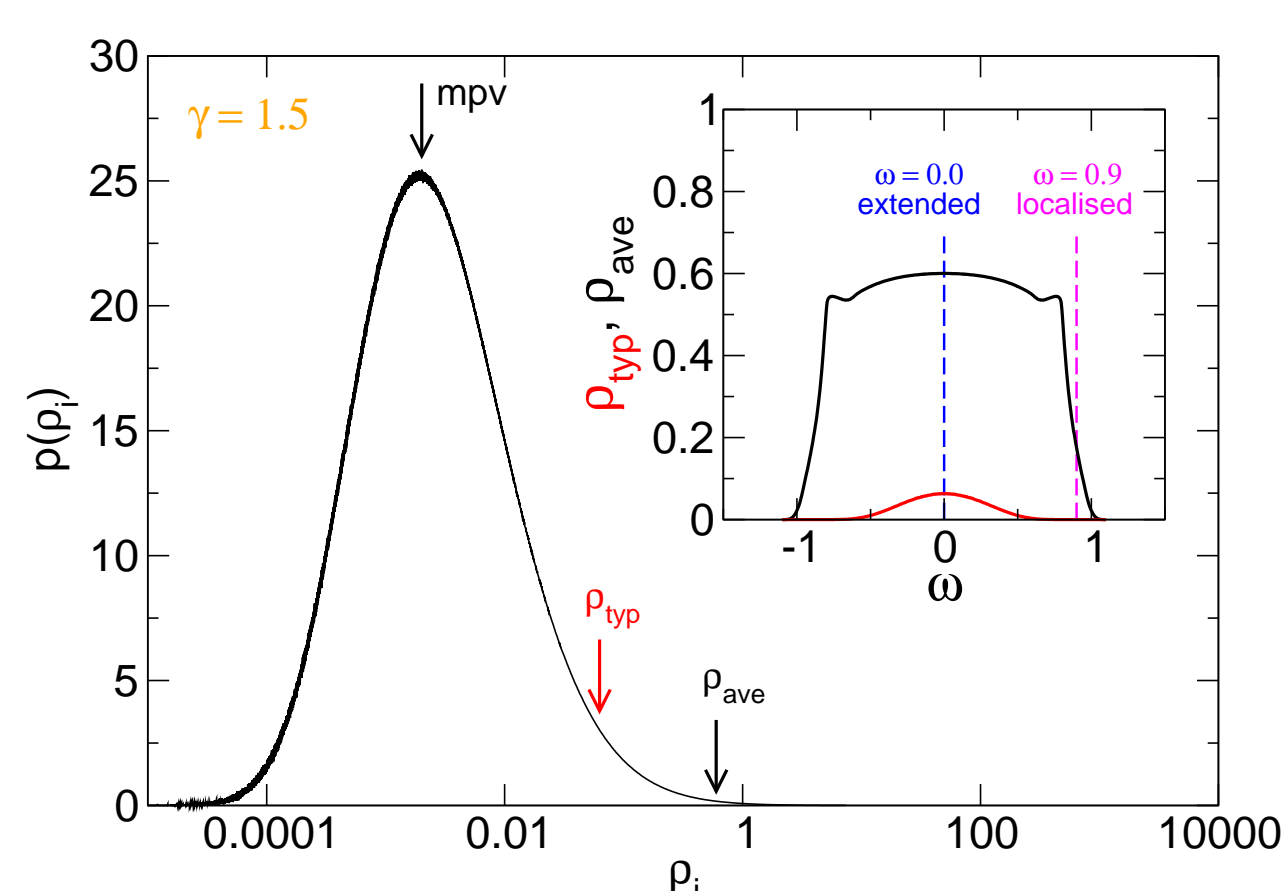
The random on-site potential ϵ_i is assumed to be uniformly distributed within $[-\gamma/2, \gamma/2]$. The bare bandwidth is set to $W_0 = 1$.

Distributions

The quantity of interest is the probability distribution of the local density of states (LDOS)

$$\rho_i(\omega) = -\frac{1}{\pi} \lim_{\eta \rightarrow 0^+} \text{Im} G_{ii}(\omega + i\eta)$$

Since the LDOS is related to the local amplitudes of the wavefunctions the transition from extended to localised states is accompanied by a qualitative change in its distribution.



Probability distribution of the LDOS for the Anderson model in the band center $\omega = 0$, for strong disorder $\gamma = 1.5 \approx 0.5 \times \gamma_{\text{crit}}$. Arrows indicate the most probable value (mpv), the typical density of states ρ_{typ} , and the averaged density of states ρ_{ave} . The inset shows $\rho_{\text{ave}}(\omega)$ and $\rho_{\text{typ}}(\omega)$ for this disorder strength. The two vertical lines indicate values of ω corresponding to localised respectively extended states (cf. next figure).

Since this critical behaviour does not manifest itself in the arithmetic mean value ρ_{ave} , different quantities must be employed to detect this transition. One possible choice is the so-called **typical density of states**

$$\rho_{\text{typ}}(\omega) = \exp\left(\frac{1}{N} \sum_i \log \rho_i(\omega)\right)$$

The AAT-method

On a Bethe lattice a selfconsistency equation

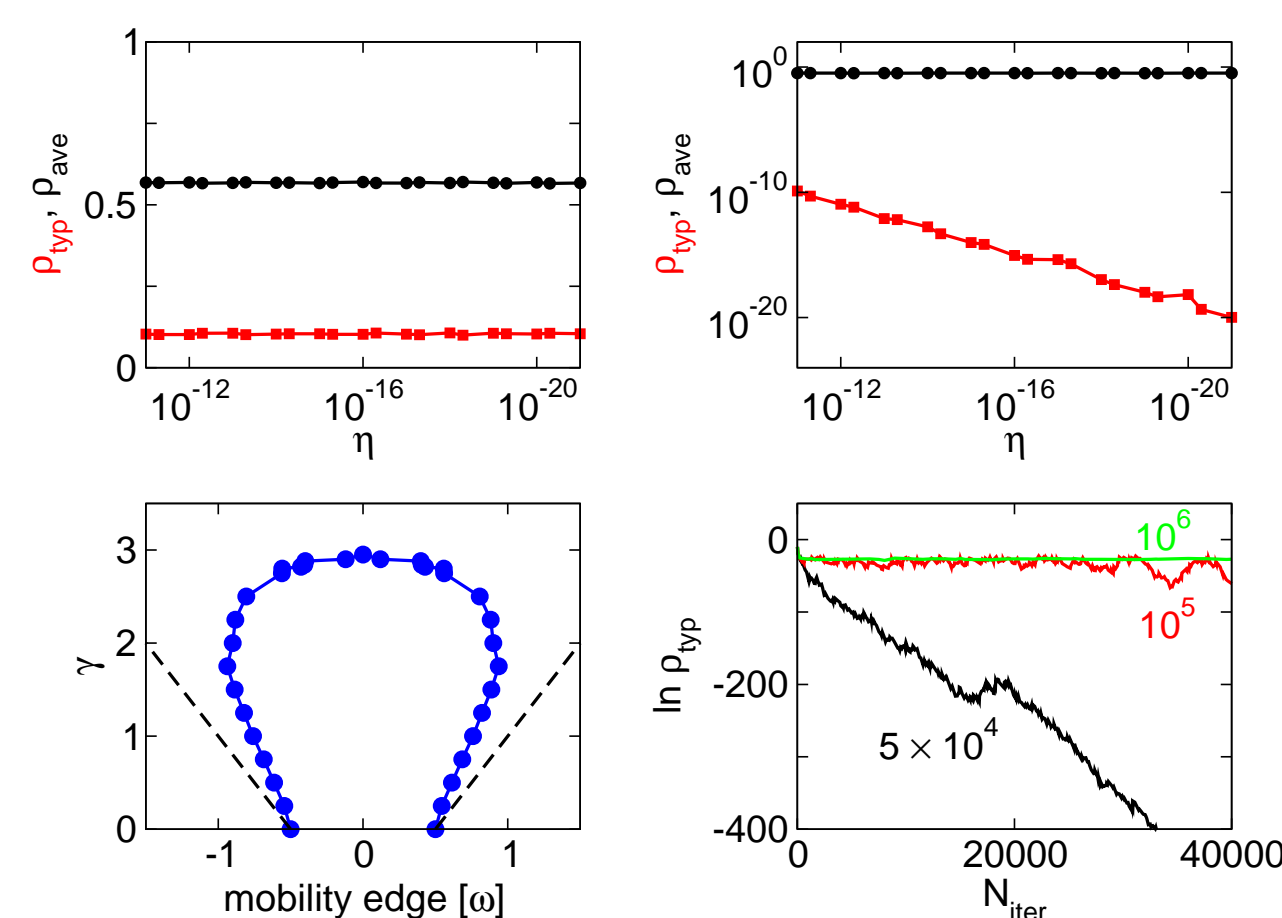
$$G_{ii}(\omega) = \frac{1}{\omega - \epsilon_i - t^2 \sum_{j=1}^K G_{jj}}$$

for the distribution of the local Green function $G_{ii}(\omega)$ can be set up following the ideas formulated by Abou-Chacra, Anderson, Thouless (AAT) [2]. The solution of this equation is obtained via a

Monte-Carlo-procedure, representing the distribution through a sample of typical 50000 up to 2.5×10^7 elements.

$\eta \rightarrow 0$ -limit

The LDOS $\rho_i = -\frac{1}{\pi} \text{Im} G_{ii}(\omega + i\eta)$, hence its distribution, is defined in the limit $\eta \rightarrow 0$. While no strict distinction between extended and localised states can be made for finite η the limiting distribution for $\eta \rightarrow 0$ exhibits clearly different features in the two regimes which can be seen in the typical density of states. Exploiting the limit $\eta \rightarrow 0$ numerically allows for a clear distinction of localised versus extended states.



The upper row displays ρ_{ave} and ρ_{typ} with respect to η for extended ($\omega = 0.0$, left picture) and localised ($\omega = 0.9$, right picture) states, with $\gamma = 1.5$. The lower left picture shows the mobility edges calculated for $\eta \rightarrow 0$ numerically, for a sample with 5×10^4 elements. The lower right picture shows ρ_{typ} versus the number of iterations N_{iter} in the Monte-Carlo procedure for sample sizes 5×10^4 , 10^5 , 10^6 .

Accordingly states at energy ω are classified as **extended** if $\rho_{\text{typ}}(\omega) > 0$, and **localised** if $\rho_{\text{typ}}(\omega) = 0$, for $\eta \rightarrow 0$. In both cases $\rho_{\text{ave}}(\omega) > 0$.

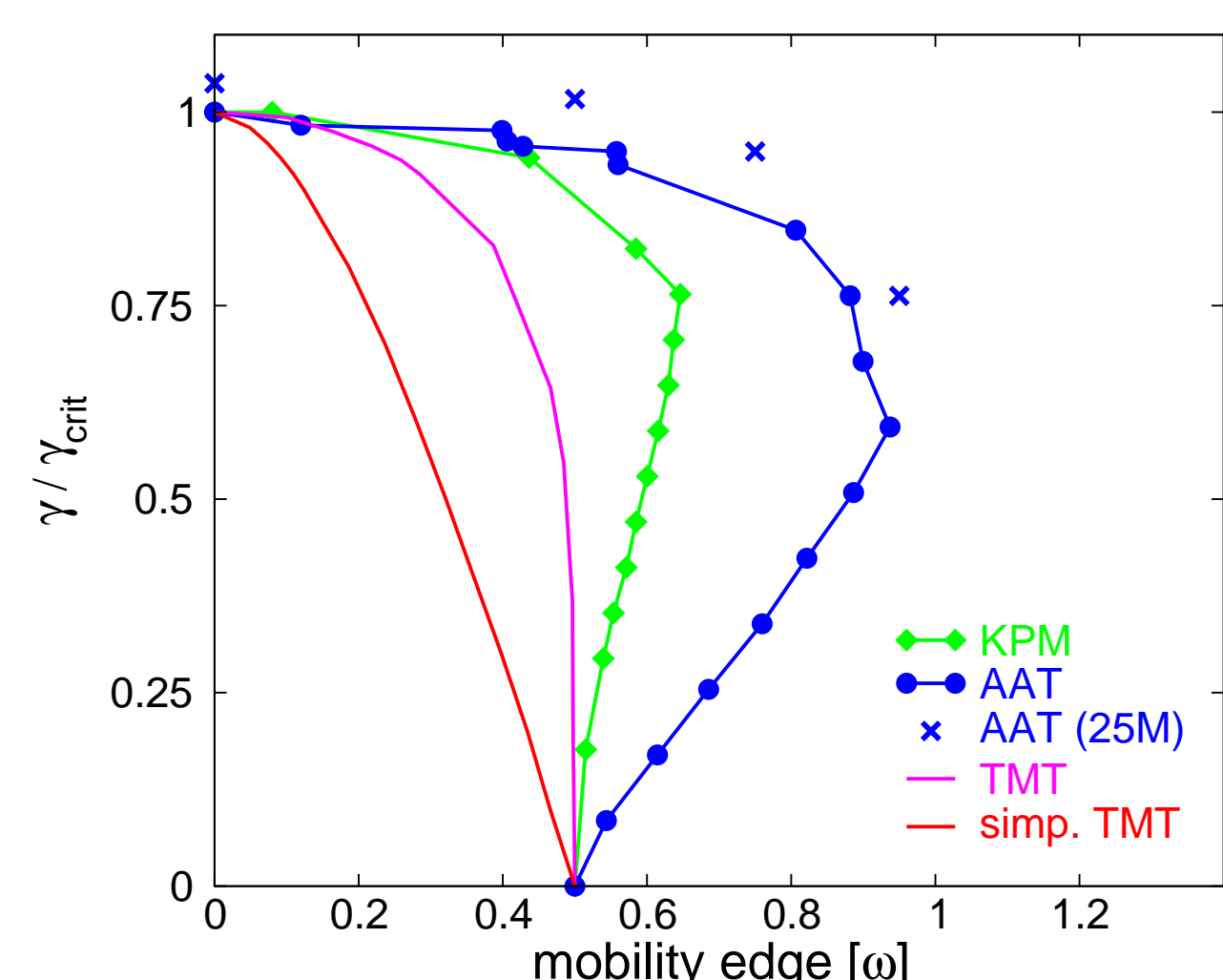
The finite size of the Monte-Carlo-sample limits the precision which the Green function's distribution is resolved with, and leads to overestimation of localisation. This limitation can be easily overcome by increasing the sample size, hence allowing for an arbitrary precise determination of mobility edges.

Averaging theories – AAT versus TMT

The previously shown results indicate that the typical (but not the averaged) density of states might play the role of an “order parameter” for localisation. The recently proposed typical medium theory (TMT) [3] tries to fully reformulate the localisation problem in terms of the typDOS, and has succeedingly been used to study Anderson localisation in the disordered Hubbard model [4]. TMT can be understood as an effective theory like the coherent potential approximation (CPA), but replacing the averaged density of states by the typical density of states, from which the system Green function is recovered through Hilbert transformation $G(\omega) = \int d\omega' \rho_{\text{typ}}(\omega') / (\omega - \omega')$.

The typDOS is dominated by small values of the local density of states which correspond to “deep” impurities. Replacing the full distribution with the typDOS thus overestimates scattering on these deep impurities and the formation of locally bound impurity states. In fact, the TMT-mobility edge resembles the one obtained by a simplified TMT-variant which only uses the minimal value of $\rho_i(\omega)$ for the maximal scattering contribution $\epsilon_i = \pm\gamma/2$. Both approaches fail to recover the reentrant behaviour of the mobility edge. This indicates that the delocalising effect due to tunneling is (mostly) neglected.

Mobility edges



Comparison of mobility edges for the Anderson model on a Bethe lattice with $K = 2$ and a cubic lattice, using different methods based on distributions. Mobility edge trajectory for the Anderson model calculated with KPM [5] for a cubic lattice (diamonds), and with AAT (circles), representing the distribution through a sample with 5×10^4 elements. The crosses indicate points in the (ω, γ) -plane, which correspond

to delocalised states if sampled with 2.5×10^7 elements. The dotted (dashed) line shows the mobility edge trajectory resulting from TMT (simplified TMT-variant).

The critical disorder for complete localisation on the Bethe lattice (with connectivity $K = 2$) is $\gamma_c \approx 2.9$. TMT (simplified TMT) gives $\gamma_c = e/2$ ($\gamma_c = 0.5$).

Anderson-Holstein model [6]

In the Anderson-Holstein-model (AHM) the electron does locally couple to dispersionless Einstein phonons.

$$H = \sum_i \epsilon_i c_i^\dagger c_i + t \sum_{\langle i,j \rangle} c_i^\dagger c_j + \Omega \sum_i b_i^\dagger b_i - \sqrt{E_P \Omega} \sum_i c_i^\dagger c_i (b_i^\dagger + b_i)$$

The “polaron” properties of this model are determined by two interaction parameters, $\lambda = E_P/2t$ and $g^2 = E_P/\Omega$, and the adiabaticity ratio $\alpha = \Omega/t$. Polaron formation sets in provided that $\lambda \gtrsim 1$ and $g^2 \gtrsim 1$. To study localisation within this interacting model the AAT scheme is combined with a DMFT-treatment of interaction, to give the statistical dynamical mean field theory (statDMFT) [7].

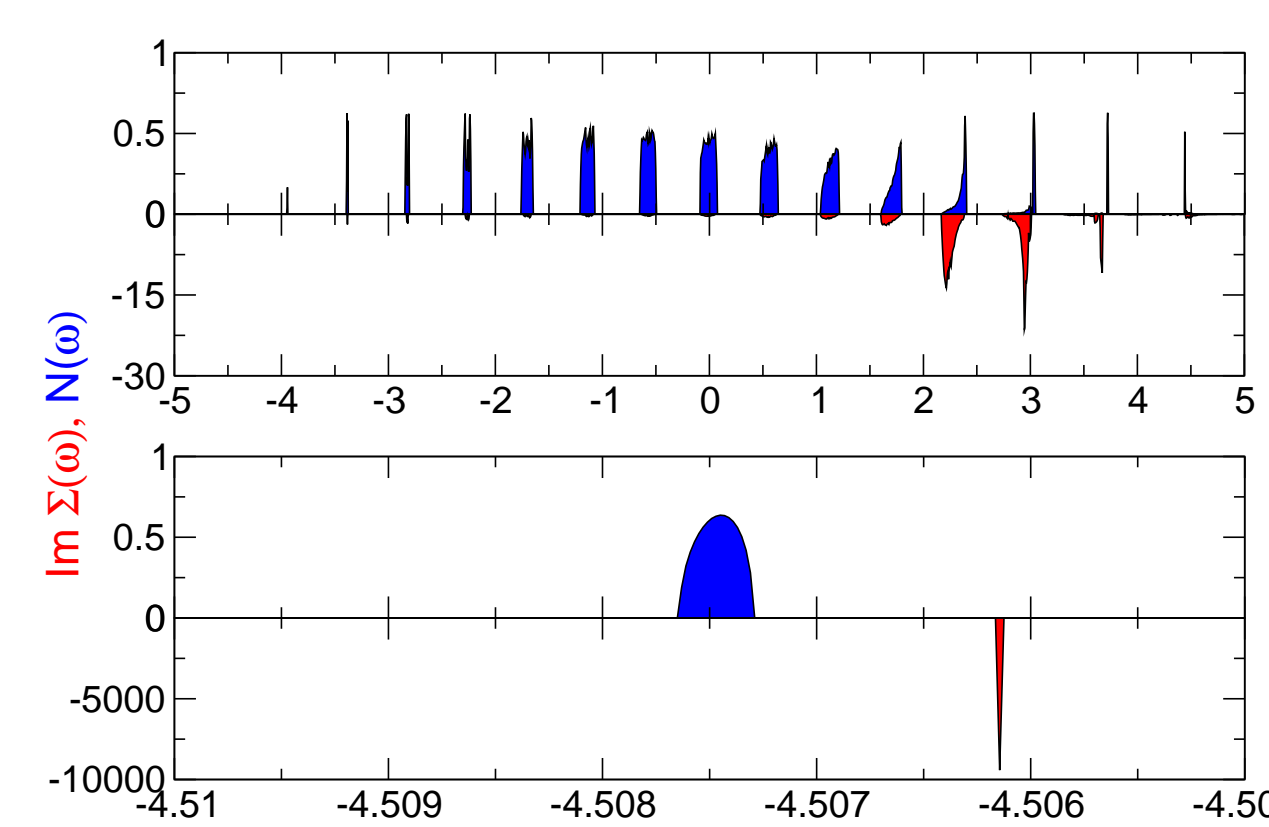
For a single polaron at $T = 0$ the DMFT-selfenergy $\Sigma_{ii}(\omega)$ can be expressed in terms of a continued fraction

$$\Sigma_{ii}(\omega) = \frac{E_P \Omega}{F_{ii}^{-1}(\omega - \Omega) - \frac{2E_P \Omega}{F_{ii}^{-1}(\omega - 2\Omega) - \dots}}$$

whose N -th level accounts for the emission and reabsorption of N (at $T = 0$ virtual) phonons. Here $F_{ii}(\omega) = (\omega - \epsilon_i - t^2 \sum_{j=1}^K G_{jj}(\omega))^{-1}$ denotes the Green's function without e-ph-interaction at site i . The Monte-Carlo-samples now contains entries for all shifted energies $\omega, \omega - \Omega, \dots$. The localisation criterion as previously introduced is still applicable.

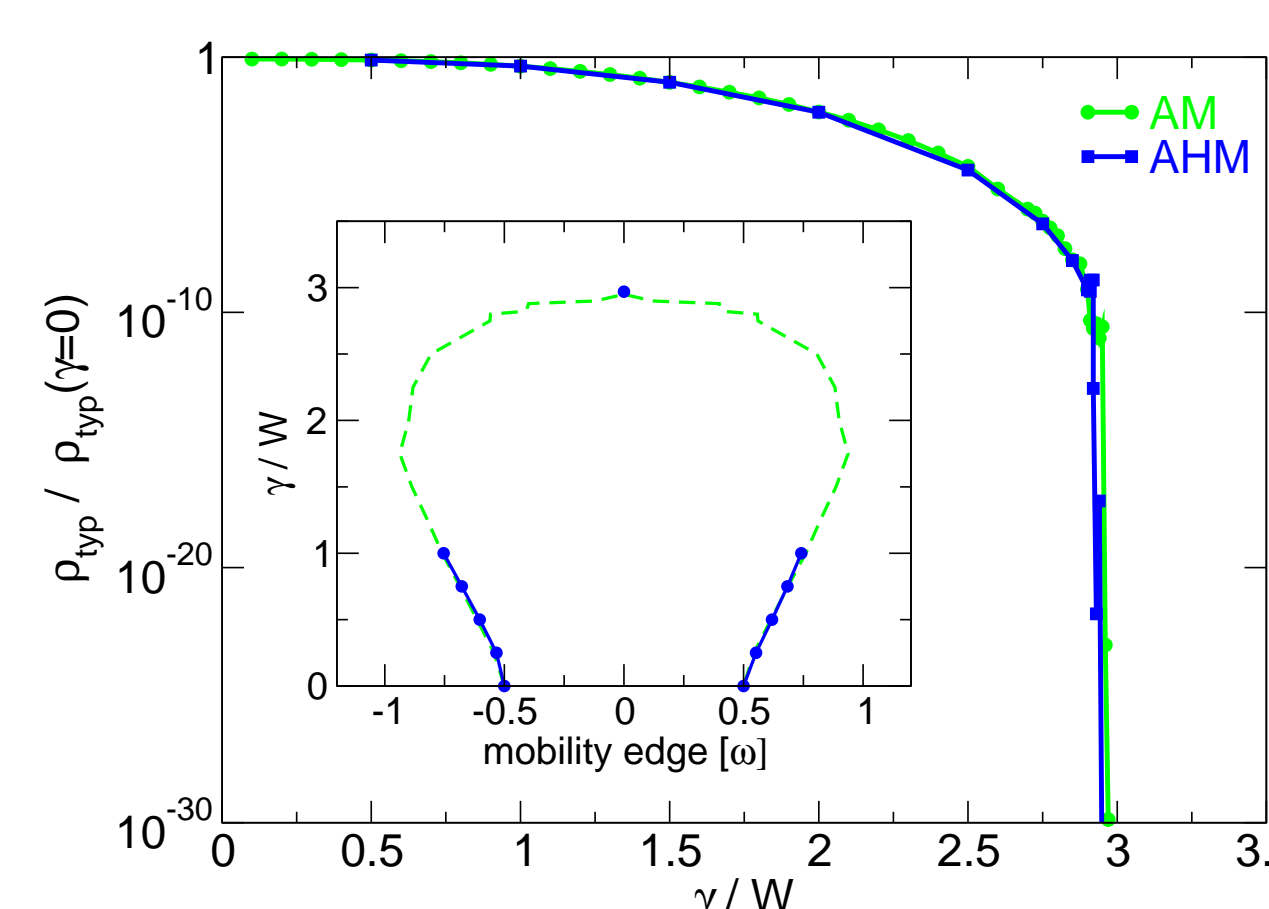
Localisation of a polaron

Antiadiabatic strong coupling



Antiadiabatic strong coupling $\tilde{\alpha} = 2.25$, $\tilde{\lambda} = 9.0$ (DMFT result). The lowest polaron subband has a renormalised bandwidth $W = 3.45 \times 10^{-4}$ and is fully coherent.

For strong coupling and large phonon frequency ($\tilde{\lambda} = 9.0$, $\tilde{\alpha} = 2.25$) the lowest polaron subband is completely coherent ($\text{Im} \Sigma(\omega) = 0$) with a rather symmetric DOS. The localisation properties of this band are expected to be same as for the pure Anderson model. As a comparison of ρ_{typ} and the mobility edge trajectories shows this is indeed the case.



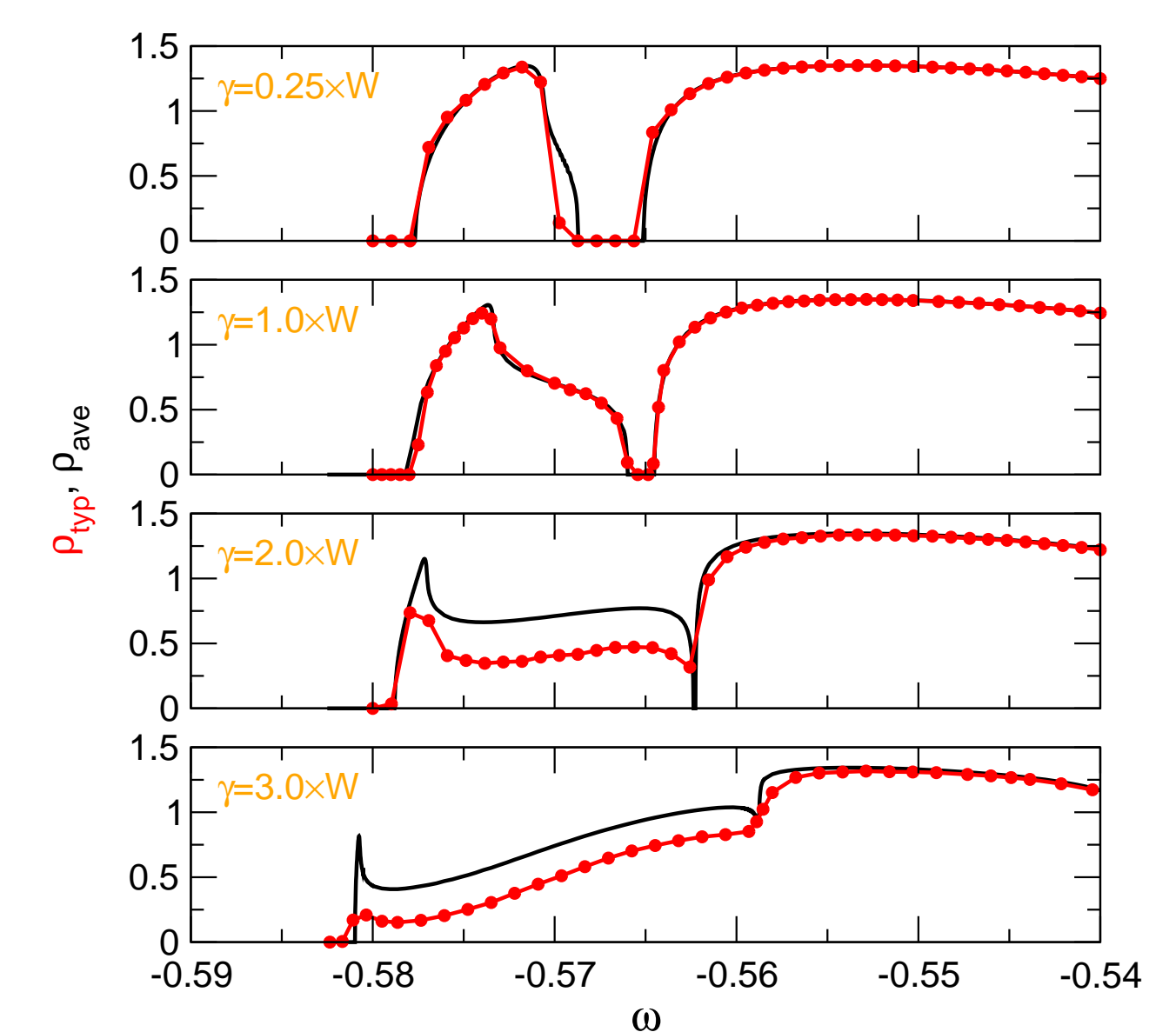
Comparison of ρ_{typ} in the bandcenter of the pure Anderson model (green curve) and the lowest polaron subband in the antiadiabatic strong coupling regime $\tilde{\lambda} = 9.0$, $\tilde{\alpha} = 2.25$ (blue curve). The respective bandwidth is denoted by W . The inset displays part of the corresponding mobility edge trajectories. The energy ω is scaled to the respective bandwidth and -center.

The two mobility edge trajectories do match even for very strong disorder when all states in the polaron

subband become localised. However the critical disorder is orders of magnitude smaller than the separation of the subbands because of the strong renormalisation of the bandwidth. So disorder can localise all states within a single subband without affecting the overall polaronic features of the system.

Adiabatic intermediate coupling

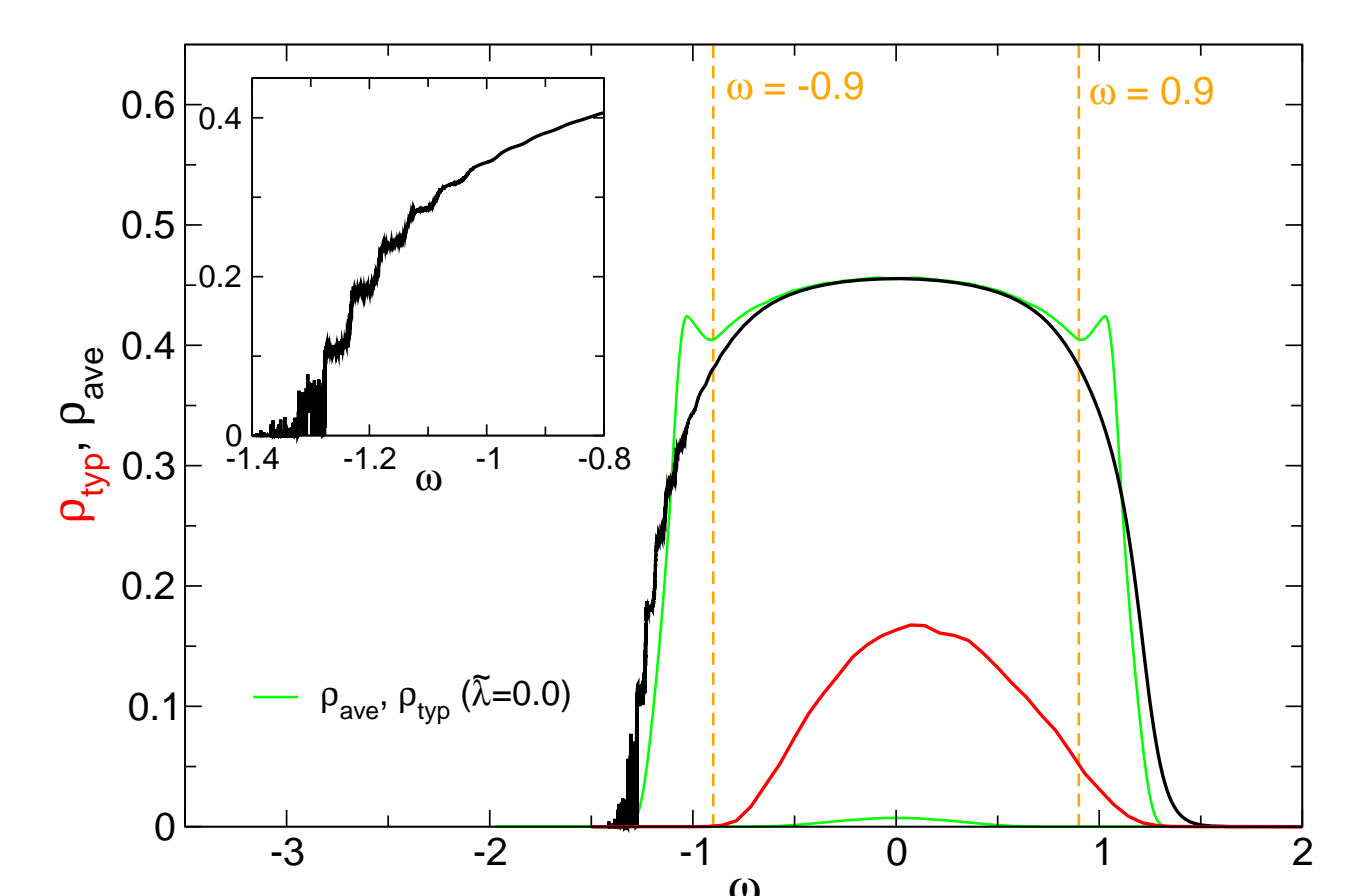
For intermediate coupling and small phonon frequency ($\tilde{\lambda} = 1.0$, $\tilde{\alpha} = 0.2$) the localisation properties of the polaron do substantially differ from that of the bare electron. States at the bottom of the lowest polaron subband are rather mobile and remain nearly unaffected for small disorder. In contrast states at the top are rather sluggish and very susceptible to disorder. Although the two lowest subbands which correspond to a different number of phonons remain separated over a large range of disorder they eventually begin to merge. The relevant energy scale changes before complete localisation of the lowest subband can occur.



ρ_{ave} and ρ_{typ} for $\tilde{\lambda} = 1.0$, $\tilde{\alpha} = 0.2$ and four values of γ . $W \approx 8.123 \times 10^{-3}$ is the width of the lowest polaron subband of the pure Holstein model ($\gamma = 0$).

Anderson regime

For $\gamma = 2$ in the pure Anderson model localised and extended states are separated by mobility edges at $\omega \approx \pm 0.9$. If electron-phonon interaction is switched on (here with $\tilde{\alpha} = 0.2$, $\tilde{\lambda} = 0.75$) states at energy ω begin to couple to states at energies less than ω (recall that $T = 0$). States at the lower mobility edge can only couple to states which are already localised. Hence disorder and e-ph-interaction work in the same direction. As a consequence polaron like defect states do form as is indicated by the step-like structure of the averaged DOS (this can be readily understood in terms of the independent boson model). At the upper mobility edge formerly localised states delocalise due to the coupling to extended states towards the band center. Here e-ph-interaction weakens the tendency towards localisation. As a consequence the upper mobility edge is shifted to higher energies.



ρ_{ave} (DMFT) and ρ_{typ} for $\tilde{\alpha} = 0.2$, $\tilde{\lambda} = 0.75$, $\gamma = 2.0$. The green curves show ρ_{ave} and ρ_{typ} for $\tilde{\lambda} = 0$. The vertical dashed lines indicate the mobility edges for $\tilde{\lambda} = 0$.

Conclusions

We reexamined how the probability distribution of the local density of states can be used for an analysis of localisation. Furthermore we studied the localisation of a Holstein polaron by means of the statDMFT and demonstrated its applicability in various parameter regimes. The results obtained clearly show that the localisation properties of a Holstein polaron are highly non universal.

References

- [1] P. W. Anderson, Phys. Rev. **109**, 1492 (1958).
- [2] R. Abou-Chacra, P. W. Anderson, and D. Thouless, J. Phys. C **6**, 1734 (1973).
- [3] V. Dobrosavljević, A. A. Pastor, and B. K. Nikolić, Europhys. Lett. **62**, 76 (2003).
- [4] K. Byczuk, W. Hofstetter, and D. Vollhardt, cond-mat/0403765 (2004).
- [5] G. Schubert, A. Weiße, and H. Fehske, cond-mat/0309015 (2003), and contribution to SCES '04.
- [6] F. X. Bronold, A. Alvermann and H. Fehske, Phil. Mag. B **84**, 673 (2004).
- [7] V. Dobrosavljević and G. Kotliar, Phys. Rev. Lett. **78**, 3943 (1997).